RSC Advances

PAPER

View Article Online
View Journal | View Issue

Cite this: *RSC Adv.*, 2026, **16**, 27256

Synthesis of sol–gel poly(ethylene glycol) coated foams for the microextraction of multiclass pesticides from apple juice samples

Apostolia Tsiasioti, [ab] Natalia Manousi, [a] Abuzar Kabir, [c] Aristidis Anthemidis [b] and Erwin Rosenberg *[a]

Received 15th February 2026
Accepted 1st May 2026

DOI: 10.1039/d6ra01360k

rsc.li/rsc-advances

To ensure food safety and fair-trade practices in fruit juices, a simple and efficient foam-in-syringe solid-phase extraction (FIS-SPE) method was developed and coupled with high performance liquid chromatography-diode array detection for multiclass pesticide monitoring. Sol–gel polyethylene glycol (Carbowax 20M) coated foams were fabricated, characterized, and evaluated as microextraction media for the first time. Key parameters influencing FIS-SPE performance were optimized. The method was validated for sensitivity, linearity, accuracy, precision, robustness, and selectivity. Environmental friendliness and practical applicability were assessed using appropriate metric tools. Under optimized conditions, relative recoveries ranged from 87% to 116%, with relative standard deviations below 12% for both intra-day and inter-day tests. Limits of detection were 0.8–1.5 ng mL^{-1}, and limits of quantification were 2.5–5.0 ng mL^{-1} for a 25 mL sample volume. The enhancement factor ranged between 11 and 38, and the absolute extraction recoveries were 21–76%. As a proof of concept, the method was applied to the analysis of various commercially available fruit juice samples, demonstrating its suitability for routine pesticide monitoring in complex food matrices.

1 Introduction

In today's health-conscious world, consumers are more and more willing to consume natural beverages that promise both nutritional value and a pleasant flavour.[1] Fruit juices are among these popular beverages owing to their health benefits and their high nutritional value. They typically contain a plethora of compounds that promote well-being or add to the particular taste, including vitamins (*e.g.*, vitamin C), sugars (like fructose, glucose, or sucrose), acids (*e.g.*, malic acid and citric acid), and minerals.[2] However, due to the ever-increasing population growth and the growing demand for agricultural products, the use of pesticides is necessary.[3] These chemicals are frequently used in pre- and post-harvest treatments to prevent fruits and vegetables from diseases, weeds, and insect damage. However, their widespread and repeated use in agriculture may pose a serious concern for the safety of food in general, and more specifically for fruit juices due to pesticide residues.[3–5]

Plants can absorb pesticides from surface water and soils through their roots and leaves. These chemicals may accumulate in the fruit pulp and become concentrated in the fruit juices.[6] In general, pesticides tend to accumulate in the pulp and the peel rather than in the fruit juice, which makes their determination more difficult in the latter since the levels at which they are found are generally low.[7] Pesticides, even at low concentrations, can adversely affect organisms by disrupting both reproductive and neurological functions. Moreover, many pesticides have been associated with mutagenicity, carcinogenicity, immuno-suppression, and cytotoxic effects.[8] Developing accurate and highly sensitive analytical methods for detecting pesticide residues in fruit juice is essential for safeguarding food safety and upholding fair practices in international trade.

Solid phase extraction (SPE) and liquid–liquid extraction (LLE) have been used for the extraction of pesticide residues from different sample matrices.[6] However, these techniques exhibit various inherent drawbacks, including the use of large amounts of solvents and/or chemicals that results in the generation of an increased volume of waste. Thus, it is necessary to improve and create better, potentially automated and more environmentally friendly solutions for sample preparation, such as many of the already known miniaturized extraction techniques.[9] To comply with the ever-increasing demands for environmental protection, it is imperative to develop analytical methods that comply with the principles of Green Analytical Chemistry (GAC)[10] and Green Sample Preparation (GSP).[11] In this context, miniaturization of the sample preparation protocol is promoted to minimize chemical

[a]*Institute of Chemical Technologies and Analytics, TU Wien, 1060 Vienna, Austria. E-mail: egon.rosenberg@tuwien.ac.at*

[b]*Laboratory of Analytical Chemistry, Department of Chemistry, Aristotle University of Thessaloniki GR-54124 Thessaloniki, Greece*

[c]*Global Forensic and Justice Center (GFJC), Department of Chemistry and Biochemistry, Florida International University, Miami, FL, USA*

consumption, waste generation, and energy demands, as well as to enhance the operator's safety. A plethora of such techniques, including solid-phase microextraction,[4] magnetic solid-phase extraction,[5] fabric phase sorptive extraction,[12] and stir bar sorptive extraction,[13] have been proposed for pesticide extraction from fruit juice samples. These sorbent-based microextraction techniques can simplify the overall analytical workflow, reduce the environmental impact of the method, and improve its selectivity.

At the same time, the development of advanced materials assists in the improvement of microextraction protocols, enhancing their versatility and efficiency, such as molecularly imprinted polymers, metal–organic frameworks, 3D printed devices, and biopolymers.[8,14,15] Towards the preparation of advanced materials, sol–gel technology can be considered as a powerful vehicle. It can be used to fabricate bulk materials and surface-bonded hybrid organic–inorganic polymer coatings with tunable selectivity and porosity. Among the other benefits of sol–gel sorbents are their increased thermal and chemical stability. In this way, sol–gel sorbents with diverse chemical properties (*i.e.*, polar, medium polar, non-polar, ion exchanger, and zwitterionic materials, *etc.*) can be prepared for the extraction of analytes with diverse properties.[16] Moreover, these materials are reusable, complying with the third principle of GSP.[11]

During the last decade, a wide range of sponge and sponge-like materials have been engineered and applied as adsorbents in diverse applications.[17–20] These materials show multiple advantages, including increased surface area, very low weight, open-pore structure, and adaptable surface chemistry that makes them appropriate for the extraction of a wide variety of target analytes from complex samples.[21] To date, sol–gel-coated foam-based microextraction media have been synthesized as practical sorbents for bisphenol A.[22] In this approach, sol–gel poly(tetrahydrofuran) (PTHF) coated foam blocks were employed as adsorbent. Moreover, the same sorbent has been utilized for the extraction of non-steroidal anti-inflammatory drugs from human urine.[23] The developed approaches exhibited the typical advantages of established microextraction techniques (regarding reduced solvent consumption, high enrichment factors, high sample throughput, and potential reusability of the sorption material) and demonstrated the benefits of sol–gel coated foams in sample preparation. However, to the best of our knowledge the utilization of sol–gel coated foams for pesticides' monitoring has not yet been reported.

In the present work, sol–gel coated Carbowax 20M (CW 20M) foam was used for the in-syringe microextraction of multi-class pesticides for the first time. High performance liquid chromatography coupled to diode array detection (HPLC-DAD) was subsequently employed for quantitative analysis of the pesticide residues. Phenyl urea herbicides (PUHs), benzoyl urea herbicides (BUHs), and triazines (TRI) were used as model analytes. The experimental parameters that can affect the performance of the microextraction scheme were thoroughly investigated. The FIS-SPE-HPLC-DAD method was validated in terms of accuracy, sensitivity, precision, selectivity, and linearity, while its green character and practicality were also examined. As a proof-of-concept, this microextraction scheme was employed for the analysis of different commercially available fruit juices.

2 Experimental section

2.1. Reagents, chemicals, and samples

Water, methanol (MeOH), and acetonitrile (ACN), all of LC-MS grade, were purchased from Honeywell (Charlotte, North Carolina, USA). Reagent grade NaCl, HPLC grade ethanol (EtOH), and HPLC grade acetone were purchased from Merck (Darmstadt, Germany). Atrazine (98.85%), terbuthylazine (99.28%), and terbutryn (99.00%) were sourced from Dr Ehrenstorfer GmbH (Augsburg, Germany). Triflumuron (99.9%), isoproturon (99.5%), linuron (99.6%), and chlorbromuron (99.4%) were purchased from Supelco (Bellefonte, PA, USA). Fig. S1 (in the SI) shows the structures of the selected pesticides. Individual stock standard solutions (500 mg L^{-1}) were prepared in MeOH, and they were stored at 4 °C. Mixtures and working standard solutions were daily prepared at appropriate concentration levels in MeOH through serial dilution of the stock standard solutions.

Open cell polyurethane blocks (20 cm × 5 cm × 2 cm) were cut into suitable cylindrical pieces prior to their coating with the sol solution by direct immersion. The materials, solvents, and chemicals used for the preparation of the sol–gel Carbowax 20M (CW 20M) coating were of analytical grade or higher. Dichloromethane, acetone, trifluoroacetic acid, CW 20M, methyltrimethoxysilane (MTMS), were purchased from Sigma-Aldrich (St. Louis, MO, USA).

Apple juice samples were collected from local supermarkets in Vienna, Austria. They were stored based on the instructions of their manufacturers, and they did not undergo any additional sample pretreatment prior to the FIS-SPE procedure.

2.2. Instrumentation

A binary HPLC system was used throughout this study, which comprised two LC-20A pumps, a DGU-20A3 solvent degassing unit, a column oven CTO-20AC, an autosampler SIL-20A, an SPD-M20A photodiode array detector, and a CBM-20A communication bus module (all from Shimadzu, Kyoto, Japan). System control and data processing were performed using LCMS Solutions software (v.3.81, Shimadzu).

A Kinetex C_{18} 100 Å (2.6 μm, 4.6 mm × 30 mm) column was used for the separation of the pesticides. The column was kept at 30 °C throughout the analysis. Gradient elution mode using water (a) and ACN (b) was used. Table S1 in the SI describes the conditions of gradient elution. The mobile phase flow rate was 1.0 mL min^{-1}, and the following retention times were obtained for the target analytes: 2.38 min for atrazine, 3.20 min for isoproturon, 4.95 min for terbuthylazine, 5.22 min for linuron, 5.58 min for chlorbromuron, 6.25 min for terbutryn, and 7.50 min for triflumuron. Finally, the quantification was performed at 210 nm for BUH (triflumuron), at 222 nm for TRI (atrazine, terbuthylazine, and terbutryn), and at 245 nm for PUHs (isoproturon, linuron, and chlorbromuron). Fig. 1 shows a representative chromatogram of a fruit juice sample that has been spiked.

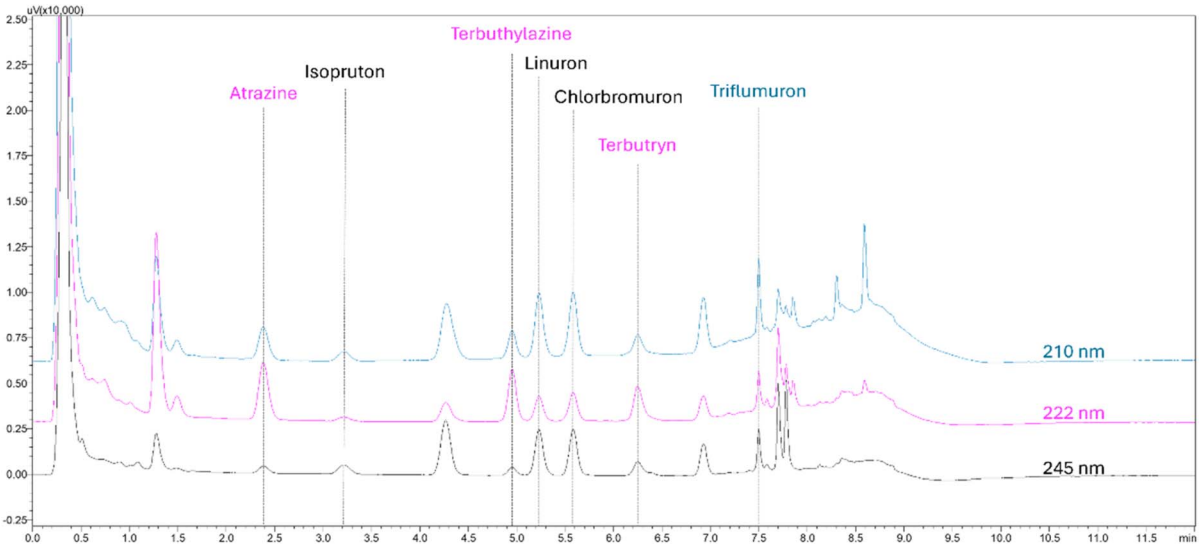

Fig. 1 Representative chromatograms of the analysis of spiked apple juice (100 ng mL^{-1}) through the FIS-SPE-HPLC-DAD method. Detection at the wavelength of maximum absorption: 210 nm: triflumuron, 222 nm: atrazine, terbuthylazine, and 245 nm: terbutryn, isoproturon, linuron, and chlorbromuron.

2.3. Fabrication of the FIS-SPE device

The preparation of the sol–gel coated foams was performed as previously reported.[22] In summary, the sol–gel CW 20 M coating solution was prepared by combining 10.0 g of CW 20 M polymer with 12.5 mL of MTMS, 25.0 mL of a methylene chloride–acetone mixture (50 : 50, v/v), and 5.0 mL of trifluoroacetic acid containing 5% water as the catalytic system. The mixture was vortexed for 3 min and centrifuged for 5 min to remove insoluble particulates. The resulting clear supernatant was transferred to a clean reaction bottle and used as the sol solution.

Foam blocks, pre-cleaned and surface-treated, were coated with the sol–gel sorbent using a dip-coating approach. For this purpose, each foam block was fully immersed in the sol solution for 4 h to allow *in situ* formation of the three-dimensional sol–gel network within the foam's porous structure. After immersion, the foams were withdrawn, gently squeezed to remove excess sol, and dried in a desiccator for 2 h. The coated foams were then aged at 60 °C for 24 h under continuous helium flow in a custom conditioning device to complete the sol–gel curing process.

Post-aging, the foams were washed with a methylene chloride–acetone mixture (50 : 50, v/v) to remove unreacted precursors and loosely bound residues, followed by drying at 60 °C for 1 h under an inert atmosphere. The finished sol–gel-coated foam sorbents were stored in sealed glass containers to prevent contamination until use.

The sol–gel CW 20M coated foams were cut into cylinders of 15 mm length and 15 mm diameter. A cylindrical piece of surface-modified foam was placed at the base of a 6 mL polypropylene syringe barrel, providing stable immobilization during solution aspiration and permitting effortless compression during dispensing. Owing to the compact structure of the foam sorbent, the use of frits was not necessary, thereby facilitating a reproducible, straightforward, and low-effort fabrication method.

2.4. Application of the FIS-SPE protocol for apple juice sample preparation

As shown in Fig. 2, activation of the foam was conducted using first 1 mL of MeOH and then 1 mL of water to remove remaining traces of organic solvent. For the extraction of the target analytes, an aliquot of 5 mL of the sample was passed through the pores of the foam and discarded through dispensation. This step was performed in 5 repetitions, each time using a fresh sample aliquot, to achieve the loading of 25 mL in total. This procedure required less than 1.0 min to be completed. Accordingly, water (1 mL) was sequentially aspirated and dispensed to wash the surface and the pores of the foam. The elution was conducted through the aspiration of 500 µL of ACN and its dispensation in three consecutive aspiration/dispensation cycles. In this case, the same aliquot of ACN was used to ensure minimum organic solvent consumption. The

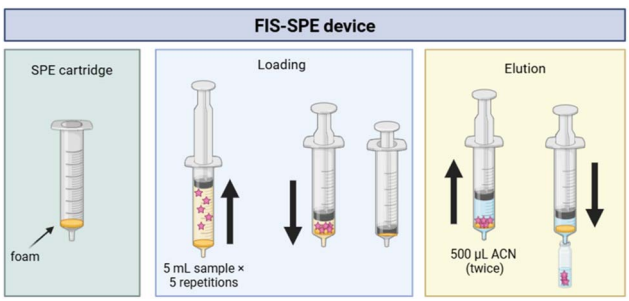

Fig. 2 Schematic representation of the operation of the proposed FIS-SPE device. Created in Biorender. Tsiasioti, A. (2026) https://BioRender.com/x83g570.

dispensed eluate was finally analyzed by HPLC-DAD. All samples were prepared in triplicate. It should be noted that during the dispensation steps, the foam was firmly compressed to remove the aspirated liquid. Following a full cycle of adsorption and elution, the foam was washed with 1 mL of MeOH and 1 mL of water until its next use.

2.5. Method development

Initially, preliminary experiments were carried out to confirm the suitability of the sol–gel CW 20 M coated foam as a sorbent for the adsorption of the selected multi-class pesticides. For these experiments, 5 mL of sample was used in the loading step and 1 mL of MeOH as the extraction solvent with two aspiration cycles. The selected pesticides contain polar functional groups, providing medium polarity characteristics that are characterized by the respective log(K_{ow}) values ranging between 2.6 and 4.9. The sol–gel CW 20 M medium has polar characteristics and has been applied for the extraction of polar and medium-polar analytes.[24] Based on this, the use of a polar sol–gel material was expected to efficiently adsorb the selected analytes based on hydrogen bonding forces and dipole–dipole interactions.

3 Results and discussion

3.1. Sorbent design and physicochemical characteristics

The sol–gel poly(ethylene glycol) (PEG)-coated foam sorbent was successfully synthesized *via* a sol–gel hydrolysis–condensation process, resulting in a chemically bonded hybrid organic–inorganic network on the porous foam substrate. The formation of a robust siloxane (Si–O–Si) framework ensured strong covalent attachment of the PEG functional layer to the substrate, thereby enhancing chemical, thermal, and solvent stability. This covalent immobilization distinguishes the present sorbent from physically coated materials and contributes to its superior durability and reusability.

The inherent open-cell structure of the foam as the inert substrate provided high permeability and a large accessible surface area, facilitating rapid mass transfer during extraction. The incorporation of PEG chains imparted hydrophilic and amphiphilic characteristics to the sorbent, enabling interaction with analytes across a wide polarity range. Such structural features are particularly advantageous for the extraction of multiclass pesticides from complex aqueous matrices such as fruit juice.

3.2. Extraction mechanism of sol–gel PEG-coated foam in FIS-SPE

The extraction of pesticides using sol–gel PEG-coated foam in foam-in-syringe solid-phase extraction (FIS-SPE) is governed by a multimodal mechanism involving partitioning and surface interactions, as illustrated in Fig. 3.

3.2.1 Partitioning into PEG phase. The dominant retention mechanism arises from the partitioning of analytes between the aqueous sample and the PEG-rich phase immobilized within the sol–gel network. PEG behaves as a quasi-liquid stationary phase, allowing analytes to distribute based on their polarity and solvation affinity. Polar and moderately polar pesticides preferentially partition into the PEG phase due to favorable dipolar interactions and hydrogen-bonding compatibility. This behavior resembles a hybrid of hydrophilic interaction liquid chromatography (HILIC) and weak reversed-phase retention mechanisms.

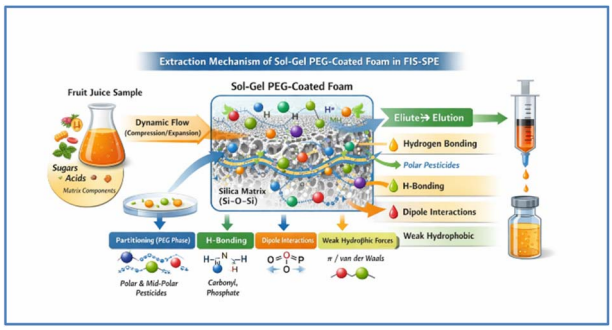

Fig. 3 Mechanism of extraction of multiclass pesticides using sol–gel PEG-coated foam in foam-in-syringe solid-phase extraction (FIS-SPE). The schematic illustrates dynamic flow-assisted extraction, highlighting partitioning into the PEG phase, hydrogen bonding, dipole–dipole interactions, and weak hydrophobic/London dispersion forces contributing to analyte retention, followed by solvent-assisted desorption.

3.2.2 Hydrogen bonding interactions. Hydrogen bonding plays a significant role in the retention of polar pesticides. The ether oxygen atoms in PEG chains act as hydrogen bond acceptors and interact with analytes containing proton-donating functional groups such as hydroxyl (–OH), amine (–NH), and amide groups. This interaction is particularly important for carbamates, organophosphorus pesticides, and benzoylurea derivatives, contributing to enhanced selectivity and extraction efficiency.

3.2.3 Dipole–dipole interactions. In addition to hydrogen bonding, dipole–dipole interactions occur between PEG chains and polar functional groups present in pesticide molecules, including carbonyl (C═O), phosphoryl (P═O), and nitrile (–CN) functionalities. These interactions facilitate the retention of mid-polar compounds such as triazines and neonicotinoids and complement the partitioning mechanism.

3.2.4 Weak hydrophobic and London dispersion interactions. Although PEG is predominantly hydrophilic, the presence of methylene (–CH_2–) groups within its backbone introduces weak hydrophobic character. This allows partial interaction with nonpolar pesticides through hydrophobic and van der Waals forces. Additionally, dispersion interactions contribute to the retention of aromatic compounds, thereby extending the applicability of the sorbent to analytes with diverse physicochemical properties.

3.2.5 Effect of dynamic flow in FIS-SPE. The FIS-SPE configuration significantly enhances extraction performance through dynamic aspiration–dispersion cycles. During operation, the foam undergoes repeated compression and expansion, promoting convective mass transfer and reducing diffusion limitations. This dynamic flow mechanism increases analyte–sorbent contact efficiency, accelerates equilibration, and results

in higher extraction recoveries compared to static extraction techniques.

3.2.6 Matrix compatibility and selectivity. Fruit juice matrices contain sugars, organic acids, and pigments that can interfere with analyte extraction. The hydrophilic PEG surface minimizes nonspecific adsorption of these matrix components, thereby reducing matrix effects and enhancing method selectivity. At the same time, specific interactions with pesticide molecules are preserved, ensuring reliable and reproducible extraction performance.

3.2.7 Adsorption capacity. In foam-in-syringe solid-phase extraction systems, adsorption capacity should be interpreted as an operational parameter reflecting the combined effects of partitioning and surface interactions under dynamic flow conditions. Unlike conventional adsorption systems governed by equilibrium isotherms, the sol–gel PEG-coated foam operates through a hybrid mechanism in which analytes distribute into a quasi-liquid PEG phase while simultaneously engaging in hydrogen bonding, dipole–dipole, and weak hydrophobic interactions. Consequently, the apparent adsorption capacity is strongly influenced by analyte polarity, flow dynamics, and sorbent accessibility rather than solely by the availability of discrete binding sites. This distinction is particularly evident in the observed dependence of recovery on $\log K_{ow}$ values, where maximum retention occurs within an optimal polarity window, highlighting the partition-dominated nature of the extraction process.

3.2.8 Desorption mechanism. Analyte desorption is achieved using organic solvents such as methanol or acetonitrile, which disrupt hydrogen bonding and dipolar interactions while favoring analyte solubility in the elution phase. The thin sol–gel coating and open porous structure enable rapid solvent penetration and efficient analyte recovery.

3.2.9 Mechanistic overview. Overall, the extraction process can be described as a synergistic combination of partitioning, hydrogen bonding, dipole–dipole interactions, and weak hydrophobic forces, further enhanced by dynamic flow conditions inherent to FIS-SPE. This multimodal mechanism enables efficient extraction of multiclass pesticides with varying polarity, making the developed method highly versatile and effective for complex food matrices.

3.3. Correlation of mechanism with extraction performance

The superior extraction performance observed for the sol–gel PEG-coated foam can be directly attributed to the interplay of the abovementioned mechanisms. Polar pesticides exhibited high recoveries due to strong hydrogen bonding and partitioning effects, while moderately nonpolar analytes were efficiently retained through combined dipolar and weak hydrophobic interactions. The dynamic flow conditions further improved extraction kinetics, resulting in rapid analysis and high enrichment factors.

These findings confirm that the developed sorbent provides a balanced interaction profile capable of accommodating a broad spectrum of pesticide chemistries, thereby validating its suitability for multiclass residue analysis in fruit juice samples.

3.4. Characterization of the polyurethane foam and sol–gel CW 20M surface coating

In order to understand surface morphology and the successful integration of sol–gel CW20M surface coating, both the pristine polyurethane foam and the sol–gel CW20M sorbent coating were extensively characterized by Fourier Transform Infrared (FT-IR) spectroscopy and Scanning Electron Microscopy (SEM).

3.4.1 Fourier Transform Infrared (FT-IR) spectroscopy. Fourier-transform infrared (FT-IR) spectra were recorded using a PerkinElmer Spectrum 100 FT-IR Spectrometer (Santa Clara, CA) equipped with a Universal ATR sampling accessory. Samples were placed directly onto the ATR crystal with uniform pressure applied to ensure consistent contact. Spectra were collected over the mid-infrared range (typically 4000–650 cm^{-1}) at an appropriate spectral resolution, and each spectrum represented the average of multiple scans to enhance signal-to-noise ratio. Background spectra were acquired prior to each measurement to correct for atmospheric contributions. The resulting FT-IR data were used to identify characteristic functional groups, evaluate chemical bonding, and confirm the successful formation of the sol–gel sorbent network.

The pertinent spectra of the sol solution ingredients and the sol–gel CW20M sorbent coated open cell polyurethane foam are shown in Fig. 4a–d.

MTMS is a precursor for the formation of the sol–gel material. Its three methoxy groups undergo hydrolysis, and the resulting products polymerize through polycondensation to form a three-dimensional siloxane network, characterized by a ≥Si–O–Si≤ backbone as a defining structural feature. Consequently, the FTIR spectrum of these precursor substances exhibit strong, broad absorption bands corresponding to the vibrational modes of Si–O and Si–O–Si. The bending vibrations of these groups contribute to absorption peaks below 900 cm^{-1}.[25]

The FTIR spectrum of pristine polyurethane foam is presented in Fig. 4a. Characteristic bands associated with the stretching vibration of the H–N bond within the urethane

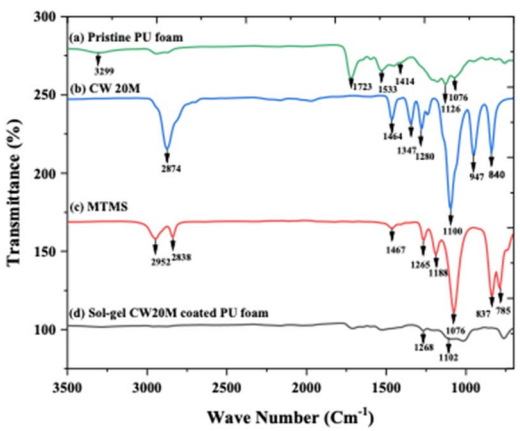

Fig. 4 FT-IR spectra of (a) pristine polyurethane foam; (b) Carbowax 20M; (c) methyltrimethoxysilane (MTMS), and (d) sol–gel Carbowax 20M coated polyurethane foam.

groups, the C=O stretching of free urethane, and the C–N stretching of the urethane group are observed at 3299, 1723, and 1533 cm^{-1}, respectively.[26]

The FTIR spectrum of CW 20M, as illustrated in Fig. 4b, exhibits an absorption peak at 2874 cm^{-1}, which can be assigned to the polymer's alkyl chain. Additional absorption bands at 1347 cm^{-1} and 1100 cm^{-1} correspond to C–H bending and C–O stretching vibrations, respectively, while the band at 1238 cm^{-1} is associated with C–H twisting vibrations.[25]

The presence of the methyl group of MTMS is confirmed through the absorption bands near 837 and 785 cm^{-1}, in addition to a strong, sharp peak at approximately 1265 cm^{-1} (Fig. 4c). Minor absorption bands near 1188 cm^{-1} and 1076 cm^{-1} are indicative of the presence of the Si–OCH_3 functional group.

The IR spectrum of the sol–gel CW 20 M-coated polyurethane foam exhibits multiple absorption bands attributable to the individual constituents of the material (Fig. 4d). Notably, the characteristic peak at approximately 1268 cm^{-1}, corresponding to the methyl functionalization of the silicon atom in MTMS, and the peak at 1102 cm^{-1}, assigned to the C–O stretching vibration of CW 20M, provide clear evidence for the successful incorporation of both sol–gel building blocks into the polyurethane foam composite.

3.4.2 Scanning Electron Microscopy (SEM) analysis. Morphological characterization of the uncoated and sol–gel-coated foam materials was performed using a Philips XL 30 Scanning Electron Microscope equipped with an EDAX detector. Foam samples were mounted on aluminum stubs using conductive carbon tape and sputter-coated with a thin conductive layer, when necessary, to minimize charging. SEM imaging was conducted under optimized accelerating voltage and magnification settings to visualize surface topography, pore structure, and the distribution of the sol–gel coating within the foam matrix. The EDAX detector enabled qualitative elemental analysis to further confirm the presence and uniformity of the sol–gel sorbent on the foam surface.

Open cell polyurethane foam is engineered with numerous interconnected pores that allow fluid to permeate easily through it. These pores tremendously expand the contact surface area for the extracting sample matrix, and therefore, polyurethane foam is considered an ideal substrate for sol–gel sorbent coating. Fig. 5 presents SEM images of pristine (uncoated) polyurethane foam and sol–gel CW 20M sorbent coated polyurethane foam. Fig. 5a and b depicts the polyurethane foam surface before sol–gel CW 20M coating at 50× and 100× magnification, respectively. The SEM images of the sol–gel CW 20M sorbent coated polyurethane foam are presented in Fig. 5c and d, which reveal relatively reduced cell opening due to the sol–gel CW 20M sorbent coating. In addition, the sponge-like porous architecture of sol–gel CW 20M sorbent has made the polyurethane surface relatively rough, as evident by the SEM images (Fig. 5c and d). This increased surface area allows rapid mass transfer from the bulk fluidic sample matrix to the sol–gel CW 20M sorbent. The same feature of the sol–gel sorbents also allows rapid elution of the extracted analytes from the sorbent.

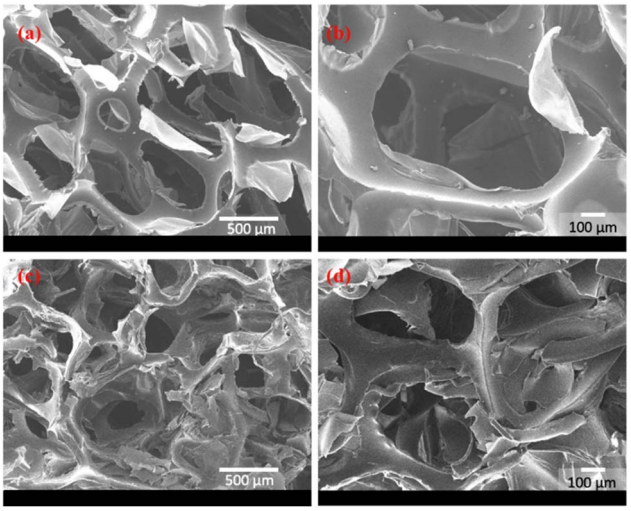

Fig. 5 SEM images of (a) uncoated polyurethane foam at 50× magnification; (b) uncoated polyurethane foam at 100× magnification; (c) sol–gel CW20M coated polyurethane foam at 50× magnification; and (d) sol–gel CW20M coated polyurethane foam at 100× magnification.

3.5. Optimization of the FIS-SPE procedure

Sol–gel CW 20 M coated FPSE media have been found to be optimal for pesticides,[27] indicating that this sorbent is appropriate for this type of analytes. Preliminary experiments showed good extraction recoveries for the target pesticides and, thus, this material was selected for method development and further optimization. To optimize the extraction process of the analytes using the sol–gel CW 20M modified polyurethane foam, the main parameters that affect the extraction were investigated. The studied parameters were the volume of the sample and the eluent, the loading cycles of the sample and the eluent, the elution solvent, and the ionic strength. All parameters were investigated independently with the OVAT ('one variable at a time') approach, that is, one parameter was optimized each time while all other parameters were kept constant, such as: 5 mL of sample with one loading cycle, 1 mL of MeOH as extraction solvent with two aspiration cycles, and 0% NaCl. Each parameter studied was expressed as normalized extraction recovery (ER%) after the comparison of the results with the optimum value, and multiplying by a factor of 100. Experiments were conducted in duplicate and both the average value and the standard deviation were calculated.

In the developed method, a polypropylene 6 mL syringe was used for packing the sorbent, and thus 6 mL was the maximum volume of sample that could be loaded in one cycle. However, since the loading-dispensing step is fast, the sample can be loaded repeatedly several times.[19] The loading-dispensing cycles of the sample were investigated by extracting the same aliquot of sample (5 mL) for 1, 2, and 5 times. Interestingly, the extraction recoveries were stable in all cases (Fig. S2(a)), indicating that one loading-dispensing cycle is sufficient for the pesticides to interact and be adsorbed by the sorbent, making it

more user-friendly. Thus, all sample aliquots were loaded on the foam sorbent in a single step without the requirement for repetition.

Subsequently, the volume of the sample was studied as it is an important factor to enhance the preconcentration. Higher volumes of samples can be used to enhance the absolute amount of analyte that is loaded onto the sorbent, enhancing the preconcentration factor.[28] In the FIS-SPE system, this can be done by aspirating/dispensing fresh aliquots of the sample. Thus, we investigated the effect of the sequential aspiration of 1, 2, and 5 fresh aliquots of 5 mL to have a sample volume of 5, 10, and 25 mL of juice, respectively. As it was found before to be the optimum, each aliquot of the sample was aspirated and dispensed one time. The extraction recoveries remained constant during the studied range (Fig. S2(b)), and the value of 25 mL (5 aliquots of × 5 mL of fresh sample) was selected since it provides a higher quantity of pesticides available to interact with the sorbent and thus a higher preconcentration of the fruit juice sample.

The elution solvent is a significant factor in order to achieve sufficient back-extraction of the absorbed analytes from the sorbent to the eluent. The selected solvent should remove the pesticides efficiently from the sorbent, and be compatible with the chromatographic system and environmentally and user-friendly. The desorption of the pesticides was studied using different elution solvents, such as methanol (MeOH), ethanol (EtOH), acetonitrile (ACN), and acetone (ACE). ACN led to the optimum desorption of the pesticides from the sol–gel CW 20 M coated foam (Fig. 6a) and was selected as the optimum.

Accordingly, the volume of the eluent was investigated to find the lowest volume of eluent needed to efficiently desorb the target analytes.[22] The eluent volume should be as low as possible as it increases the preconcentration factor, but at the same time, it should be sufficient to achieve complete desorption of the analytes. The eluent volume was examined within the range 300–1500 μL, with the results reported in Fig. 6b. An increase in the extraction efficiency was observed by increasing the eluent volume from 300 to 500 μL. This could be attributed to the incomplete desorption of the analytes at the low level of 300 μL. However, further increase did not provide any further improvement, indicating that 500 μL is sufficient to elute the analytes. Therefore, the volume of 500 μL was selected as the optimum one, ensuring method greenness.

Next, the number of aspiration/dispensing cycles of the elution solvent was investigated to find the optimum number of repetitions that are necessary to elute the retained pesticides. For this purpose, the same aliquot of ACN was used. In this way, the preconcentration factor was maintained as high as possible, while the minimum organic solvent consumption was ensured. Thus, one to five consecutive aspiration/dispensing cycles of the

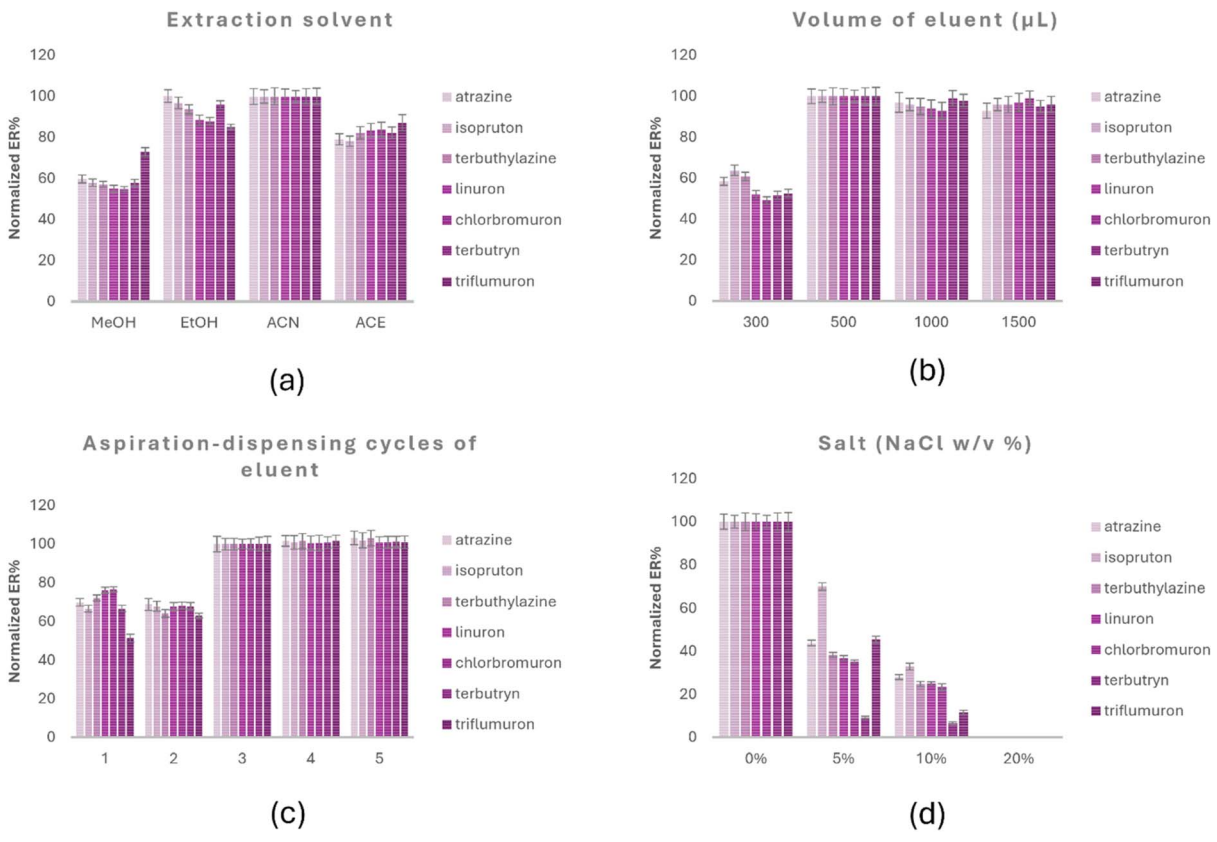

Fig. 6 Normalized ER% (average of two repetitions ± standard deviation) for the optimization of the main parameters of the FIS-SPE process: (a) extraction solvent, (b) elution volume, (c) number of loading-dispensing cycles of the eluent, and (d) salt content ($n = 3$).

eluent were investigated. The extraction recoveries were improved by increasing the number of cycles from one to three (Fig. 6c). One and two aspiration/dispensing cycles were found to be insufficient to back-extract the retained pesticides. No further increase was observed when elution was performed in five consecutive cycles, indicating that three repetitions were enough for the complete desorption of the analytes. Thus, three aspiration/dispensing cycles of ACN were finally selected for the elution step.

Furthermore, the ionic strength is an important factor in the optimization of the adsorption of polar or medium-polar analytes to the sorbent. The ionic strength affects the extraction process through two distinct phenomena. In the first case, known as salting-out effect, the solubility of the analytes is decreased in the matrix, and thus the interactions of the analytes with the functional groups of the sorbent are increased. However, in the second case, the ions enhance at high electrolyte concentration the sample's viscosity, reducing the mass transfer of the analytes towards the sorbent. NaCl was added to the sample, as a model electrolyte, at variable amounts (*i.e.*, 0–20% w/v). As can be observed in Fig. 6d, the recovery values decreased significantly by enhancing the ionic strength. This can be possibly attributed to the fact that the electrostatic interaction increased between the salt ions and organic compounds, and hindered the mass transfer of the pesticides or blocked the active sites of the sorbent.[29] Therefore, no salt addition was selected for the further study.

3.6. Performance of the FIS-SPE-HPLC-DAD method

The analytical figures of merit were studied for the determination of pesticides in fruit juices. The method was validated according to International Council for Harmonization (ICH) guidelines in terms of selectivity, linearity, limit of detection and quantification (LOD and LOQ), precision, and accuracy.[30] For the assessment of selectivity, six blank samples ($n = 6$) were analyzed. As shown in the chromatograms (Fig. 1), there are no interfering peaks co-eluting with the target analytes, proving the selectivity of the method. The absence of interferences can be attributed to the combination of the selectivity of HPLC as separation technique, DAD detection, and sorbent extraction. To evaluate the linear range, a series of calibration standards was prepared by spiking elevated concentrations of standard solutions in organic apple juice. Each concentration level was analyzed in triplicate ($n = 3$). The analytical signals were used for plotting the calibration curves through least-squares linear regression analysis. The analytical figures of merit are shown in Table 1. The linearity of the method was found satisfactory, and the coefficients of determination (r^2) were higher than 0.992 in all cases. The LOQ values were determined as the lowest points on the calibration curves, while the LOD values were calculated by dividing the LOQ values by 3.3. Thus, the LOQs of the target analytes were found to be in the range 2.5–5.0 ng mL^{-1}, while the LODs ranged between 0.8 and 1.5 ng mL^{-1}. The maximum residue limits (MRLs) of the target analytes are between 0.01 and 0.05 mg kg^{-1} for the apple fruit, and they are also considered applicable for the juice product, as no MRL values are set for this matrix. Therefore, the sensitivity of the method is considered sufficient for the monitoring of pesticides in apple juice samples.[31]

Pre-concentration factor (PF) is a coefficient that expresses how many times the concentration of the analyte increases.[32] The PF was determined by dividing the initial sample volume (25 mL) by the final volume (500 μL), yielding a value of 50. The enhancement factor (EF) was defined as the ratio between the calibration slopes obtained before and after the FIS-SPE procedure. The EFs were found in the range of 11–38. The extraction recovery (ER%) is evaluated by comparing the EF of each analyte with the PF of the method.[33] The ER% of the pesticides were 21–76%.

The accuracy and precision of the analytical method were assessed using spiked organic apple juice ($c = 25.0$ and 250 ng mL^{-1}), as no certified reference materials were available. Intra-day accuracy and precision were determined from three consecutive measurements ($n = 3$), while the inter-day values were assessed through three measurements on three different working days ($n = 3 \times 3$). The experimental results are shown in Table S2. The accuracy was expressed as relative recovery (RR%) and calculated as the ratio of the found to the added concentration of the spiked samples. The precision was calculated as the relative standard deviation (RSD%). The accuracy of the method was satisfactory, with RR% being in the range 86.6 to 115.9% for intra-day and 85.9 and 106.5% for inter-day accuracy. The RSD values were calculated in the range 4–10% and 4–12% for intra- and inter-day, respectively, indicating good precision of the proposed method.

Finally, the robustness of the method was evaluated in terms of slight intentional variations of the following parameters: amount of sample, amount of eluent, and sponge dimensions (height). All the experiments were conducted individually,

Table 1 Analytical figures of merit of the proposed protocol for pesticide analysis by HPLC-DAD with FIS-SPE sample preparation

Analyte	Regression analysis	r^2	Linear range (ng mL^{-1})	LOD (ng mL^{-1})	LOQ (ng mL^{-1})	ER%	EF
Atrazine	$y = 320(\pm3)x + 694$ (±505)	0.9995	2.5–250	0.8	2.5	23	12
Isoproturon	$y = 65(\pm1)x + 204$ (±75)	0.9997	2.5–250	0.8	2.5	22	11
Terbuthylazine	$y = 241(\pm3)x + 1007$ (±347)	0.9995	2.5–250	0.8	2.5	55	28
Linuron	$y = 210(\pm2)x - 202$ (±257)	0.9997	2.5–250	0.8	2.5	70	35
Chlorbromuron	$y = 205(\pm2)x + 319$ (±303)	0.9995	2.5–250	0.8	2.5	76	38
Terbutryn	$y = 187(\pm4)x + 445$ (±537)	0.9981	2.5–250	0.8	2.5	31	16
Triflumuron	$y = 99(\pm4)x + 7524$ (±634)	0.9924	5.0–250	1.5	5.0	21	11

modifying one parameter at a time at an analyte concentration level of 75 ng mL^{-1}. Table S3 summarizes the experimental results. As can be observed, the effects of the above experiments resulted in acceptable fluctuations in the extraction performance, ranging between 95 and 105%. Thus, the proposed FIS-SPE-HPLC-DAD method shows good robustness.

3.7. Correlation between extraction recovery and the polarity of the pesticides

The polarity ($\log K_{ow}$) of the selected pesticides varies widely from 2.6 (polar) to 5.6 (nonpolar). The $\log K_{ow}$ values of atrazine, isoproturon, terbuthylazine, linuron, chlorbromuron, terbutryn and triflumuron are 2.6, 2.9, 3.1, 3.2, 3.1, 3.7 and 5.6, respectively. The extraction recovery (ER%) values are presented in Table 1.

The observed extraction behaviour demonstrates a clear dependence on analyte hydrophobicity, where absolute recovery increases with $\log K_{ow}$ values from 2.6 to approximately 3.2, corresponding to improved partitioning into the PEG phase and enhanced intermolecular interactions. However, further increases in hydrophobicity, as observed for terbutryn ($\log K_{ow}$ 3.7) and triflumuron ($\log K_{ow}$ 5.6), result in decreased recovery. This deviation can be attributed to a mismatch between analyte polarity and sorbent characteristics, where highly hydrophobic compounds exhibit reduced affinity for the moderately polar PEG phase. Additionally, steric hindrance and increased molecular size limit diffusion into the sol–gel network, while reduced hydrogen bonding capacity further diminishes interaction strength. In the case of triflumuron, extensive fluorination and bulky aromatic structure exacerbate these effects, leading to poor extraction efficiency. These findings confirm that sol–gel PEG-coated sorbents operate within an optimal polarity window, favouring the extraction of moderately hydrophobic analytes while exhibiting reduced performance for both highly polar and highly nonpolar compounds.

3.8. Evaluation of the method's greenness and practicality

The green character of the developed method was evaluated using the Complementary Green Analytical Procedure Index (ComplexGAPI)[34] and Blue Applicability Grade Index (BAGI).[35] The openly available software tools were used to create their respective pictograms. The results are shown in Fig. 7a and b, respectively, alongside the description of the individual parts. ComplexGAPI is a green metric tool that evaluates the sample pretreatment and preparation, chemicals, instrumentation, method type, and new material preparation (*i.e.*, the sol–gel coated foam) in terms of their environmental impact. From the evaluation, a pictogram is obtained, divided into different sections for different criteria of the assessment. A color code of green, yellow, and red shows low, acceptable, or high environmental impact. Table S4 shows the attributes of ComplexGAPI evaluation alongside their justification. The proposed approach exhibits green merits (Fig. 7a), which can be attributed to the miniaturized extraction scheme that results in low chemical consumption and reduced waste generation. Moreover, the synthetic route for the preparation of the coated foam is also green since it results in high yield, does not require further purification, requires only a common setup, and is performed under hermetic sealing.

Finally, the practicality of the method was examined.[35] BAGI is a metric tool that focuses on the "blue" principles of analytical chemistry, which are related to its practical aspects.[36] In BAGI, the sample preparation and the instrumental analysis are simultaneously examined. An asteroid pictogram is obtained, divided into sub-sections that correspond to the evaluation parameters. These sections can be dark blue, blue, light blue, and white colored revealing high, medium, low, and no practicality. A numerical score is also obtained for comparative purposes between different analytical methods. Typically, a BAGI score of 60.0 or higher is recommended. Table S5 shows the attributes of BAGI evaluation alongside their justification. As can be observed, the herein proposed FIS-SPE protocol

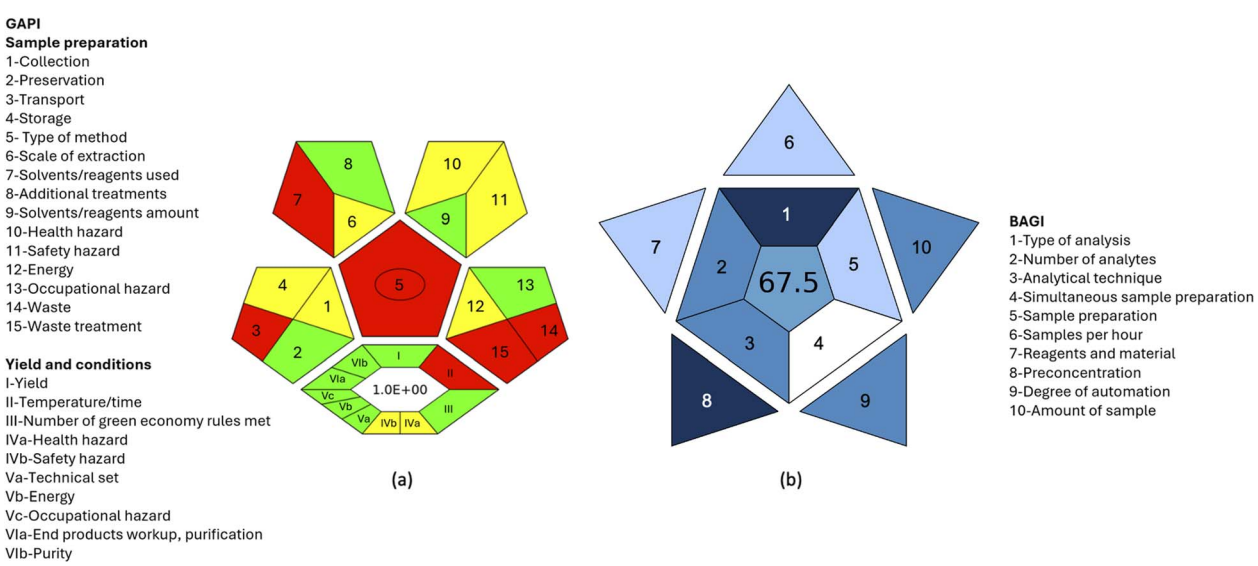

Fig. 7 ComplexGAPI (a) and BAGI (b) pictograms of the FIS-SPE-HPLC-DAD method.

Table 2 Comparison of the FIS-SPE-HPLC-DAD method with other HPLC protocols for the determination of the selected categories of pesticides in fruits and fruit juice samples

Pesticides	Sample preparation	Extraction (adsorption) time (min)	Sample volume (mL)	RR%	RSD%	EF	Preconcentration	LOD (ng mL^{-1})	Ref.
Triazine pesticides									
Cyanazine, atrazine, propazine, and terbuthylazine	Magnetic dispersive micro-solid phase extraction	0.3	30	80.1–90.6	<6.5 (intra)	120–136	Magnetic dispersive liquid–liquid microextraction	0.3	37
Cyanazine and atrazine	Effervescence-assisted dispersive liquid–liquid microextraction	2	8	77.28–101.13	<5.16 (intra)	137.83, −156.70	No	0.05–0.06	38
Simazine, atrazine, prometryn, terbuthylazine, propazine	Fabric phase sorptive extraction	30	10	91.8–108.8	<5.6 (intra), <8.8 (inter)	36.7–51.8	Evaporation/ reconstitution	0.15	12
Ametryn, atrazine, and terbutryn	Supported liquid membrane extraction	30	100	N.A.	<10.68 (intra)	2.8–4.9	No	2.61–12.32	39
Simazine, atrazine, and propazine	Dispersive magnetic solid phase extraction	30	10	80.1–108.4	<5.2 (intra), <5.2 (inter)	9.8–9.9	Evaporation/ reconstitution	0.5–1.0	40
Atrazine, terbuthylazine, terbutryn	FIS-SPE	<1 min	25	92 – 110	<8 (intra), <12 (inter)	12–40	No	1.5	This study
Benzoylurea pesticides									
Diflubenzuron, triflumuron, hexaflumuron, and teflubenzuron	SPE	50	50 g[a]	85.5–112.7	<6.8 (intra)	500	No	0.02–0.05	41
Diflubenzuron, chlorfluazuron, flufenoxuron, hexaflumuron, triflumuron	Dispersive liquid–liquid microextraction with deep eutectic solvents	2	8	76.87–101.1	<3.57	N.A.	No	0.3–0.6	42
Diflubenzuron, hexaflumuron teflubenzuron	Floated organic drop microextraction	25	15	88.49–96.21	<3.47	N.A.	No	5.0–10.0	43
Diflubenzuron, triflumuron, hexaflumuron, and flufenoxuron	Pipette vial dispersive liquid–liquid microextraction	—	8	91.4–110.9	<2.5 (intra), <2.6 (inter)	147–206	No	0.03–0.28	44
Triflumuron	FIS-SPE	<1 min	25	92 – 106	<8 (intra), <9 (inter)	20	No	3.0	This study
Phenylurea pesticides									
Linuron	Effervescence-assisted dispersive liquid–liquid microextraction	2	8	72.18–109.15	<4.62	153.85	No	0.16	38
Thidiazuron and forchlorfenuron	Ultrasound-assisted dispersive-filter extraction	1	25 g[a]	86.8–96.8	<5.4 (intra), <7.1 (inter)	N.A.	Evaporation/ reconstitution	1.0–1.25 ng g^{-1}	45
Monuron, chlorotoluron, and monolinuron	In-syringe temperature-controlled liquid–liquid microextraction	Approx. 5	8	97.29–103.56	<4.90 (intra), <5.16 (inter)	N.A.	No	0.25–2.59	46
Monuron, chlortoluron, isoproturon, and monolinuron	Dispersive liquid–liquid microextraction using supramolecular solvent	Approx. 5	10	81.21–113.12	<4.99 (intra), <5.98 (inter)	37.1–72.8	No	0.13–0.19	47
Linuron, isoproturon, chlorbromuron	FIS-SPE	<1	25	87–116	<10 (intra), <12 (inter)	8–26	No	1.5	This study

[a] Sample mass (g)

exhibited a score of 67.5, showing good practicality. This can be attributed to the different classes of analytes included in the study, the common instrumentation, the good, obtained sensitivity, the selection of miniaturized extraction, and the semi-automation using common devices (Fig. 7b).

3.9. Reusability of the sol–gel CW 20 M coated foam

The performance of the sol–gel CW 20 M coated foam was evaluated in terms of reusability for the adsorption of pesticide traces in juices. According to the principles of GSP, reusable materials are preferred, setting reusability as an important factor for the development of microextraction methods.[11] For this reason, the sol–gel CW 20 M coated foam was used in thirty-five consecutive extractions of the selected analytes using spiked apple juice ($c = 50.0$ ng mL^{-1}). It should be noted that, after each cycle, the sorbent was washed with methanol and water to remove endogenous substances that might have been retained by the sorbent. After the extraction cycles, the RR% values for the target PUHs were calculated in the range 91–98% (Fig. S3). This indicates that the sol–gel CW 20 M–coated foam can be reused at least thirty-five times for monitoring pesticides in fruit juice samples.

3.10. Comparison with published methods

A comparison of the herein presented approach was conducted with other reported methods for the determination of different classes of pesticides: TRI, BUHs, and PUHs. Sorbent-based and solvent-based extraction techniques were selected that have been used for the extraction of the selected pesticides from fruits and fruit juice samples. Among the sorbent-based techniques, a wide variety of materials have been used, including magnetic biochar, sol–gel zwitterionic sorbent, quantum dots and mesoporous carbon embedded in imprinted polymer, covalent organic framework sorbent, and monolithic sol–gel capsules. Each of these techniques suits the specific needs of the analytical procedure and supports the advancement of sorbent materials towards selectivity and environmental impact. Magnetic biochar provides a high specific surface area, a rich pore structure, and strong hydrogen bonding interactions, increasing the adsorption efficiency. The zwitterionic sorbent combines non-polar, acidic, and basic groups for the efficient extraction of pesticides and cleaning the acidic interferences from fruit samples. Quantum dots and mesoporous carbon provide a high surface area incorporated to molecularly imprinted polymer that contains specific binding sites complementary to the target analytes. Finally, covalent organic frameworks and monolithic sol–gel sorbents are porous materials that increase the adsorption of the pesticides in the active sites.

The results of the comparison are presented in Table 2. As can be observed, the proposed method has acceptable results in terms of accuracy, precision, and sensitivity in comparison to the other methods. Moreover, enhancement factors of more than one order of magnitude are obtained without the need for additional preconcentration steps (*e.g.*, evaporation/reconstitution). This ensures handling simplicity, reduced sample preparation time, and reduced sources of errors. It should be noted that the proposed method is an effective tool for the simultaneous determination of multi-class pesticides in a single step in a short time using a simple extraction device. Overall, the results reveal that the proposed protocol is efficient for the monitoring of different pesticide residues in fruit juices.

3.11. Application to the analysis of fruit juice samples

As a proof-of-concept, the developed FIS-SPE-HPLC-DAD method was applied for the determination of the selected analytes in apple juice samples obtained from local supermarkets ($n = 6$). As can be seen in Table S6, the selected pesticides were not detected in the examined samples. Spiked samples were also prepared at a concentration level of 25 ng mL^{-1}. As can be observed, relative recoveries (RR%) were satisfactory, ranging between 84.8 and 117.6%. Fig. S4 displays the chromatograms of the analysis of a blank and a spiked juice sample. The above results indicate the applicability of the proposed method in fruit juice analysis.

4 Conclusions

In this work, a novel FIS-SPE protocol was proposed as a front-end to HPLC-DAD for the determination of multi-class pesticide residues in apple juice. This novel approach combines the inherent advantages of the sol–gel sorbents, such as high extraction efficiency, with the advantages of the versatility and handling simplicity of foam sorbents. The enhancement factors were up to 38, and the extraction recoveries were up to 76%. Good environmental friendliness and practical applicability (BAGI score of 67.5) were obtained. Moreover, good accuracy (RR: 87–116%), precision (RSD <12%), and sensitivity (LODs: 0.8–1.5 ng mL^{-1}) were achieved. The main limitation of the study is that the sorbent is not currently commercially available, and it has to be synthesized in the lab. However, in one synthetic procedure, large amounts of coated foam can be produced at once, making this appropriate for a high number of analyses. The proposed method is particularly attractive due to the reduced use of chemicals, the rapid microextraction procedure, and its high sample throughput, the negligible back-pressure when percolating the sample, and the reusability of the composite foam material. Due to the tunable nature of the sol–gel coated foams, materials with different properties (*e.g.*, polar, non-polar, medium polar, *etc.*) can be synthesized and used in food analysis depending on the properties of the target analytes. Therefore, future perspectives of this study include creation of foams with different properties for the extraction of a wide range of analytes from complex environmental, biological, and food samples. All things considered, the coated foams can serve as a powerful microextraction sorbent for analytical chemists to ensure food safety.

Author contributions

Apostolia Tsiasioti: data curation, formal analysis, investigation, methodology, validation, visualization, writing – original

draft, Natalia Manousi: conceptualization, formal analysis, investigation, methodology, writing – original draft, Abuzar Kabir: conceptualization, data curation, formal analysis, investigation, methodology, resources, writing – original draft, writing – review & editing, Aristidis Anthemidis: conceptualization, investigation, resources, writing – review & editing, Erwin Rosenberg: conceptualization, investigation, resources, project administration, supervision, visualization, writing – review & editing.

Conflicts of interest

There are no conflicts to declare.

Data availability

The authors confirm that the data supporting the study findings are available within the manuscript. Raw data that support these findings are available from the corresponding author upon request.

Supplementary information (SI) is available. See DOI: https://doi.org/10.1039/d6ra01360k.

Acknowledgements

The authors acknowledge TU Wien Bibliothek for financial support through its Open Access Funding Programme.

References

1 Q. Zhang, J. Zhao, R. Xie, W. Xiao, X. Mao, C. Yuan, Y. Wang and Y. Wan, *Microchem. J.*, 2023, **187**, 108392.
2 G. Tyagi, D. K. Jangir, P. Singh, R. Mehrotra, R. Ganesan and E. S. R. Gopal, *J. Food Sci. Technol.*, 2014, **51**, 476–484.
3 S. Ahmadi, S. Khazaei and F. mehri, *J. Food Compos. Anal.*, 2024, **128**, 106012.
4 S. Cortés-Aguado, N. Sánchez-Morito, F. J. Arrebola, A. G. Frenich and J. L. M. Vidal, *Food Chem.*, 2008, **107**, 1314–1325.
5 L. Du, X. Wang, T. Liu, J. Li, J. Wang, M. Gao and H. Wang, *Microchem. J.*, 2019, **150**, 104128.
6 B. Jin, L. Xie, Y. Guo and G. Pang, *Food Res. Int.*, 2012, **46**, 399–409.
7 J. L. Tadeo, C. Sánchez-Brunete, B. Albero and L. González, *Crit. Rev. Anal. Chem.*, 2004, **34**, 165–175.
8 A. Arena, M. Zoccali, A. Ferracane and L. Mondello, *TrAC, Trends Anal. Chem.*, 2024, **180**, 117911.
9 J. Płotka-Wasylka, N. Szczepańska, M. de la Guardia and J. Namieśnik, *TrAC, Trends Anal. Chem.*, 2015, **73**, 19–38.
10 A. Gałuszka, Z. Migaszewski and J. Namieśnik, *TrAC, Trends Anal. Chem.*, 2013, **50**, 78–84.
11 Á. I. López-Lorente, F. Pena-Pereira, S. Pedersen-Bjergaard, V. G. Zuin, S. A. Ozkan and E. Psillakis, *TrAC, Trends Anal. Chem.*, 2022, **148**, 116530.
12 N. Manousi, V. Alampanos, I. Priovolos, A. Kabir, K. G. Furton, E. Rosenberg, G. A. Zachariadis and V. F. Samanidou, *Food Chem.*, 2022, **373**, 131517.
13 Z. Ayazi and R. Jaafarzadeh, *Chromatographia*, 2017, **80**, 1411–1422.
14 D. Olorunnisola, C. G. Olorunnisola, C. Günter, C. P. Okoli, M. O. Omorogie, E. I. Unuabonah, H. M. Rawel and A. Taubert, *RSC Adv.*, 2025, **15**, 32796–32809.
15 S. B. Hosseinian, M. Ghani and J. B. Raoof, *Adv. Sample Prep.*, 2025, **16**, 100215.
16 A. Kabir and V. Samanidou, *Mol*, 2021, **26**, 865.
17 M. Maggira, E. A. Deliyanni and V. F. Samanidou, *Molecules*, 2019, **24**, 2086.
18 T. Chatzimitakos, V. Samanidou and C. D. Stalikas, *J. Chromatogr. A*, 2017, **1522**, 1–8.
19 M. Ghani, R. M. Frizzarin, F. Maya and V. Cerdà, *J. Chromatogr. A*, 2016, **1453**, 1–9.
20 M. Shirani, E. Parandi, H. R. Nodeh, B. Akbari-adergani and F. Shahdadi, *Food Chem.*, 2022, **373**, 131421.
21 T. G. Chatzimitakos and C. D. Stalikas, *Molecules*, 2020, **25**, 1–20.
22 N. Manousi, I. Priovolos, A. Kabir, K. G. Furton, V. F. Samanidou and A. Anthemidis, *Anal. Chim. Acta*, 2023, **1268**, 341400.
23 N. Manousi, A. Tsiasioti, A. Kabir, A. Anthemidis and E. Rosenberg, *Microchem. J.*, 2025, **219**, 116147.
24 A. Tartaglia, M. Locatelli, A. Kabir, K. G. Furton, D. Macerola, E. Sperandio, S. Piccolantonio, H. I. Ulusoy, F. Maroni, P. Bruni, F. Croce and V. F. Samanidou, *Mol*, 2019, **24**, 382.
25 B. Jain, R. Jain, A. Kabir, N. Ali, M. Rashid Khan and S. Sharma, *J. Chromatogr. B:Anal. Technol. Biomed. Life Sci.*, 2024, **1247**, 124327.
26 Y. Dulyanska, L. Cruz-Lopes, B. Esteves, R. Guiné and I. Domingos, *Polymers*, 2024, **16**, 1–12.
27 N. Manousi, V. Alampanos, A. Ferracane, G. Efstratiadis, A. Kabir, K. G. Furton, P. Q. Tranchida, G. A. Zachariadis, L. Mondello, E. Rosenberg and V. F. Samanidou, *J. Chromatogr. A*, 2022, **1672**, 463026.
28 F. Maya, C. Palomino Cabello, J. M. Estela, V. Cerdà and G. Turnes Palomino, *Anal. Chem.*, 2015, **87**, 7545–7549.
29 X. He, T. Sun, L. Wang and X. Jiang, *J. Chromatogr. B:Anal. Technol. Biomed. Life Sci.*, 2021, **1163**, 122499.
30 ICH Q2(R2), *Validation of analytical procedures – Scientific guideline | European Medicines Agency (EMA)*, https://www.ema.europa.eu/en/ich-q2r2-validation-analytical-procedures-scientific-guideline, accessed 11 March 2026.
31 *EU Pesticides Database – MRLs – Pesticide residue(s) and maximum residue levels (mg/kg)*, https://ec.europa.eu/food/plant/pesticides/eu-pesticides-database/start/screen/mrls/details?lg_code=EN&pest_res_id_list=385&product_id_list=, accessed 16 March 2026.
32 S. Yılmaz, B. Hazer and M. Tuzen, *Food Chem.*, 2024, **457**, 140114.
33 N. Altunay, B. Hazer, M. Farooque Lanjwani, M. Tuzen, H. Ul Haq and G. Boczkaj, *Food Chem.*, 2023, **425**, 136523.
34 J. Płotka-Wasylka and W. Wojnowski, *Green Chem.*, 2021, **23**, 8657–8665.
35 N. Manousi, W. Wojnowski, J. Płotka-Wasylka and V. F. Samanidou, *Green Chem.*, 2023, **25**, 7598–7604.

36 P. M. Nowak, R. Wietecha-Posłuszny and J. Pawliszyn, *TrAC, Trends Anal. Chem.*, 2021, **138**, 116223.
37 X. Zheng, X. Guo, Y. Zhang, J. Han, X. Jing and J. Wu, *Food Chem.*, 2025, **468**, 142430.
38 A. Legesse, N. Megersa and B. S. Chandravanshi, *Anal. Chim. Acta*, 2025, **1333**, 343400.
39 N. Megersa and S. Kassahun, *Food Addit. Contam.,:Part A*, 2012, **29**, 789–798.
40 N. Phirisi, J. Płotka-Wasylka and O. Bunkoed, *J. Chromatogr. A*, 2024, **1726**, 464977.
41 Y. Song, R. Ma, L. Hao, X. Yang, C. Wang, Q. Wu and Z. Wang, *J. Chromatogr. A*, 2018, **1572**, 20–26.
42 X. Liu, M. Chen, Z. Meng, H. Qian, S. Zhang, R. Lu, H. Gao and W. Zhou, *J. Chromatogr. B*, 2020, **1140**, 121995.
43 J. Zhou, R. Liu, G. Song and M. Zhang, *Anal. Lett.*, 2009, **42**, 1805–1819.
44 X. Xi, M. Yang, G. Shen, X. Wu, R. Lu, W. Zhou, S. Zhang and H. Gao, *J. Sep. Sci.*, 2016, **39**, 391–398.
45 Y. Yuan, Y. Han, D. Han, C. Yang and H. Yan, *Food Control*, 2020, **118**, 107417.
46 W. Xu, J. Li, J. Feng, Z. Wang and H. Zhang, *J. Chromatogr. B*, 2021, **1174**, 122721.
47 S. Chen, Y. Jiang, J. Li, M. You, R. Zhang, J. Li, Z. Fu, J. Xie and Z. Wang, *Food Chem.*, 2024, **450**, 139298.